

Supporting Information

Exfoliated Monolayer GeI₂: Theoretical Prediction of a Wide-Band Gap Semiconductor with Tunable Half-Metallic Ferromagnetism

Chun-Sheng Liu*, Xiao-Le Yang, Jin Liu, and Xiao-Juan Ye*

Key Laboratory of Radio Frequency and Micro-Nano Electronics of Jiangsu Province,
College of Electronic and Optical Engineering, Nanjing University of Posts and
Telecommunications, Nanjing 210023, China

*E-mail: csliu@njupt.edu.cn (C.-S.L.)

*E-mail: yexj@njupt.edu.cn (X.-J.Y.)

I. The structural and electronic properties of bulk GeI₂

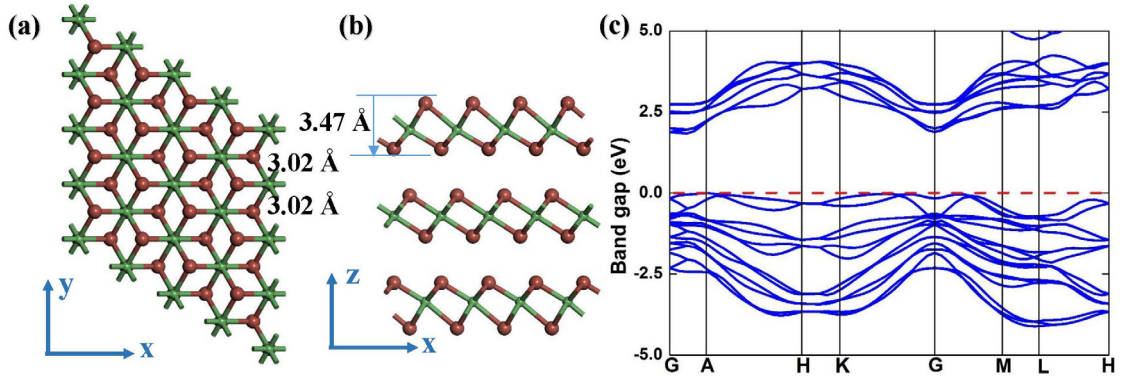


Figure S1. The optimized bulk GeI₂ structure in top a) and side b) views. c) The band structures of bulk GeI₂ with HSE+SOC functional.

II. Molecular dynamics simulations of monolayer GeI₂

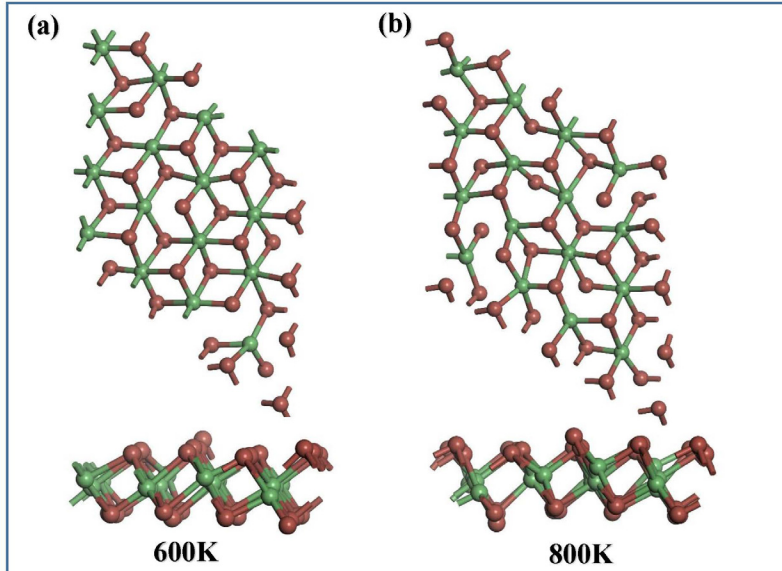


Figure S2. The snapshots of top and side views of the final atomic configurations at a) 600 and b) 800 K.

III. In-plane stiffness (C_{2D})

C_{2D} is defined as $(E - E_0)/S_0 = C_{2D}(\Delta l/l_0)^2/2$, where E_0 is the total energy of cell without dilation and S_0 is the equilibrium lattice area. The strain step of this data calculation is 0.5%. The relationship between $\Delta E = E - E_0$ and $\Delta l/l_0$ is shown in Figure S3. According to our computation, the in-plane stiffness C_{2D} of monolayer GeI₂ is 30.79 (30.80) N/m along the a (b) direction.

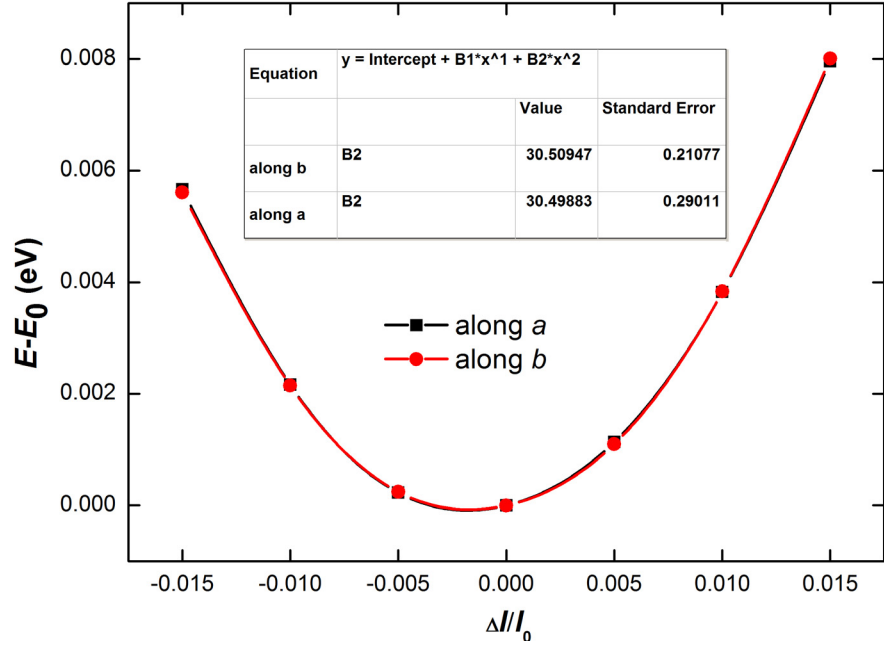


Figure S3. The total energy shift $E-E_0$ as a function of lattice deformation $\Delta l/l_0$ along a and b directions of monolayer GeI_2 .

IV. The electronic properties of multi-layered GeI_2 systems

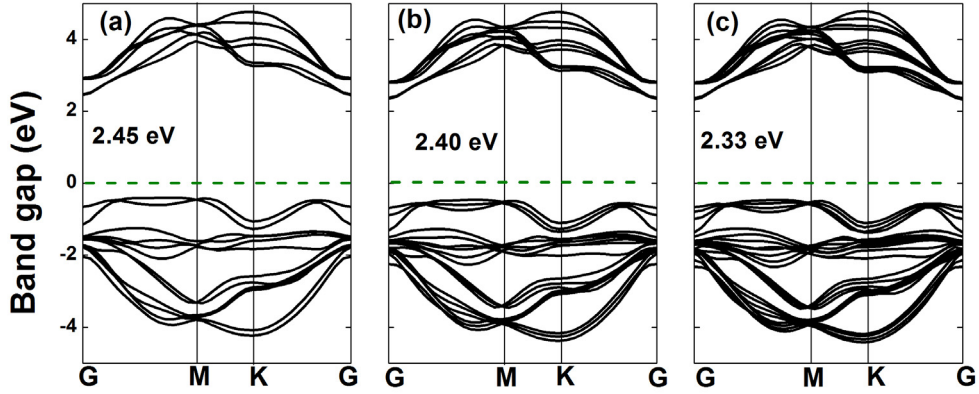


Figure S4. The band structures of (a) bi-, (b) three-, and (c) four-layered GeI_2 systems from HSE06+SOC functional.

V. Carrier mobility

According to the deformation potential (DP) theory, the carrier mobility of 2D materials can be estimated by the following expression:

$$\mu = \frac{e\hbar^3 C_{2D}}{K_B T m_i^* m_d (E_1^i)^2}$$

where \hbar , K_B , T , and m^* are the reduced Planck constant, Boltzmann constant,

temperature (300 K), and effective mass, respectively. m_i^* ($i = h$ for holes, $i = e$ for electrons) is based on the effective mass approximation $m^* = \hbar^2 (\partial^2 E / \partial K^2)^{-1}$. The effective masses along the a (b) direction are 0.25 (0.28) m_0 for electron and 0.72 (0.44) m_0 for hole. The average effective mass m_d is determined by $m_d = \sqrt{m_x^* m_y^*}$. The deformation potential constant E_1 is defined by $\frac{\Delta V}{\Delta l / l_0}$, which represents the energy of CBM for electrons and the VBM for holes along the transport (a and b) direction. ΔV is the energy change (conduction band or valence band) under certain strain. The l_0 is the lattice constant along the transport direction, and Δl is the deformation of l_0 . The relationship between E_1 and dilation $\Delta l / l_0$ is shown in Figure S5. The deformation potentials (E_1) are -6.31 (-6.37) eV for electron and -3.60 (-5.49) eV for hole along the a (b) direction, respectively.

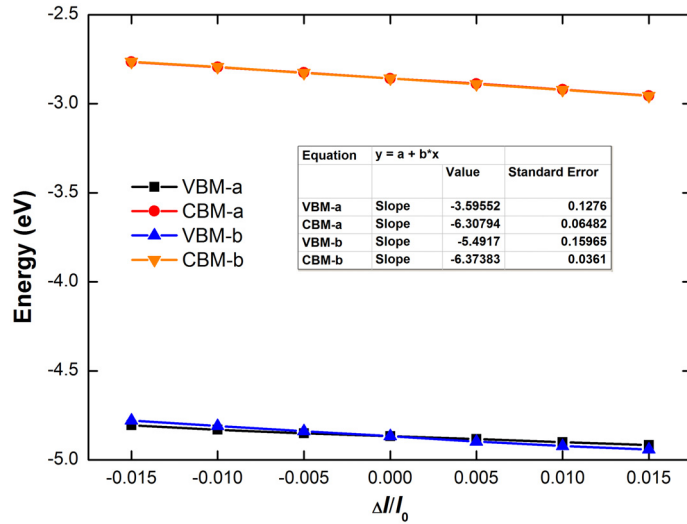


Figure S5. The relationship between the energy shift of the band edge position with the dilation $\Delta l / l_0$.

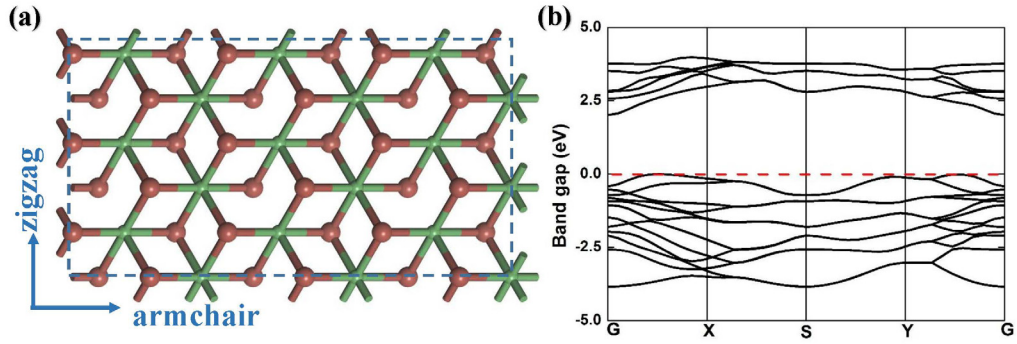


Figure S6. (a) The structure of monolayer GeI_2 with the rectangular supercell. (b) The band structure of its rectangular supercell.

VI. The deformation charge density, phonon spectrum, magnetism orders, and band structure of GeI_2H

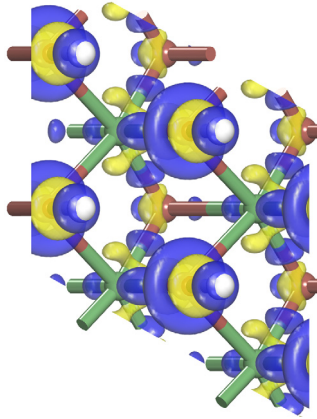


Figure S7. The deformation charge density plots of GeI_2H . The iso-surface value is $0.015 \text{ e}\text{\AA}^3$. The yellow and blue areas represent the electron depletion and accumulation regions, respectively.

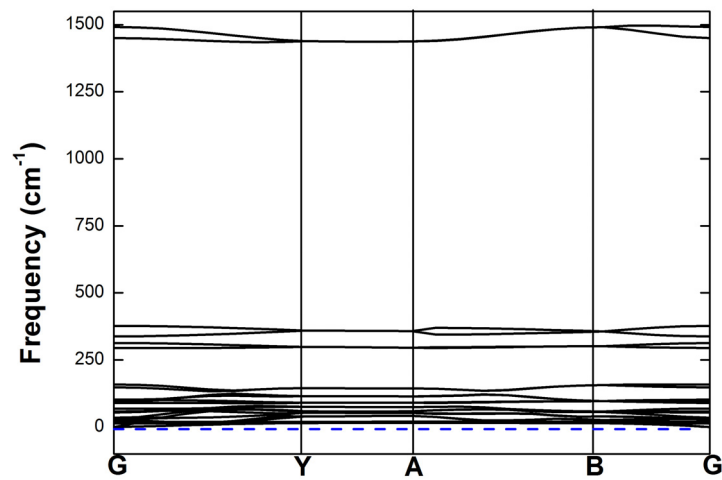


Figure S8. The phonon spectrum of hydrogenated GeI_2 .

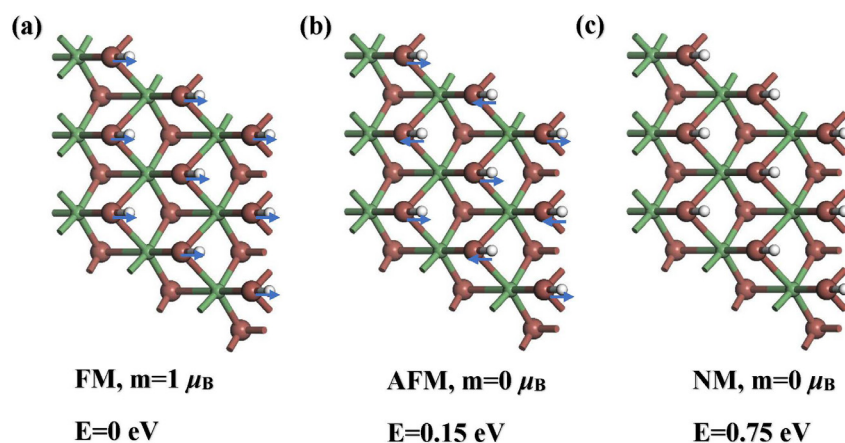


Figure S9. Three magnetic configurations of hydrogenated GeI_2 , including the magnetic moments and their relative energies with respect to the FM state for a) FM, b) AFM, and c) NM states.

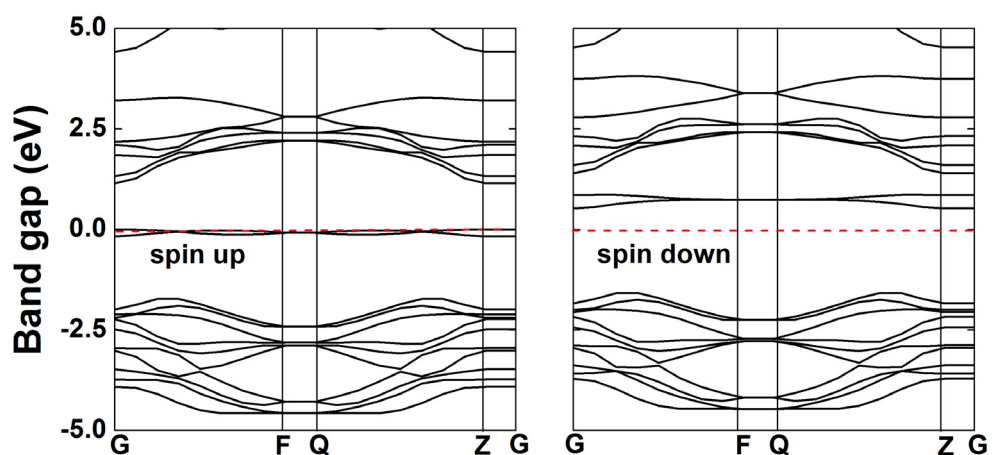


Figure S10. The spin-up and the spin-down band structures of GeI_2H .